Level-of-Detail Digitization of High Ceilings in Virtual Reality

Jacob Edwards[ID], Stephen D. Laycock[ID], Thomas Roebuck[ID], Yingliang Ma[ID], Cheng Wang[†][ID]

University of East Anglia, United Kingdom

Figure 1: *Our Level-of-Detail (LOD) framework enables efficient digitization of high heritage ceilings, demonstrated through the 4.8-meter-high historical ceiling (37.5m length) at the National Trust's Blickling Hall, United Kingdom. Our approach combines 3D Gaussian Splatting (3DGS) [KKLD23] reconstruction with high-resolution 3D scannings of intricate emblematic patterns, creating a hybrid visualization system in Virtual Reality (VR). The VR environment enables seamless transitions between architectural-scale visualization and immersive inspection of fine details, enhanced by integrated narrative storytelling.*

Abstract
The digitization of elevated ceilings featuring intricate 3D patterns in heritage settings presents significant challenges due to their substantial height and constrained accessibility. To address this, we propose a hybrid Level of Detail (LOD) framework that synergizes 3D Gaussian Splatting (3DGS) for rapid base reconstruction with targeted 3D scanning of regions of interest (ROIs). First, 3DGS is used to rapidly generate a low-LOD, real-time navigable model of the entire ceiling. Second, accurate 3D scanning of selected ROI captures fine surface details. This two-stage workflow significantly reduces processing time compared to full-structure scanning while preserving spatial context, enabling seamless transitions between broad-scale exploration and immersive inspection of high-fidelity fragments. Validated through a case study at the National Trust's Blickling Hall, a 17th-century gallery with a 37.5-meter-long and 4.8-meter-high ceiling, our method demonstrates scalable potential for heritage conservation, offering a blueprint for balancing reconstruction efficiency with immersive engagement.

CCS Concepts
• *Computing methodologies* → *3D Reconstruction; Shape Modeling; Virtual Reality;*

1. Introduction

Cultural heritage sites face mounting threats from environmental decay and human activity, necessitating innovative solutions for preservation and public engagement. At the National Trust's Blickling Estate, the 400-year-old Long Gallery ceiling (37.5 meters in length and 4.8 meters in height), a masterpiece of Renaissance plasterwork by Edward Stanyon [Gap98], exemplifies this challenge. Its intricate emblematic designs, inspired by Henry Peacham's Minerva Britanna (1612) [Pea12] (see Sec. 2), are increasingly vulnerable to structural cracking and material degradation. This project addresses two interconnected goals: Creating a high-fidelity 3D digital record of the ceiling's emblematic patterns in distant placement, and developing a VR system to enable immersive public interaction with these otherwise inaccessible details. By integrating computational advances in 3D reconstruction and VR, we aim to establish a scalable framework for heritage conservation and storytelling.

Level of Detail (LOD), a cornerstone of computer graphics, optimizes rendering by dynamically adjusting model complexity based

---

† Corresponding author, Cheng.C.Wang@uea.ac.uk

on contextual relevance [HD04]. Traditionally applied to real-time systems like gaming or simulations, LOD prioritizes computational efficiency through geometric simplification (e.g., mesh decimation, texture downsampling) while maintaining perceptual coherence [LRC*02]. In this work, we re-purpose LOD's core philosophy, balancing efficiency and fidelity, for heritage digitization, but invert its paradigm: instead of simplifying existing high-resolution data, we strategically combine low-cost rapid reconstruction with targeted high-precision scanning with the key aim to reduce the model acquisition time whilst preserving regions of interest (ROIs) with high-quality 3D scanning methods.

Our method is a hybrid workflow for scalable detail operating in two stages, tailored to the constraints of the ceiling environment:

- 3D Gaussian Splatting (3DGS) [KKLD23] for Base Reconstruction: Using 3DGS, we generate a low-LOD model of the entire ceiling (37.5 meters in length at Blickling Hall) which can be rendered in real time, even under distant viewing condition. This coarse representation captures global geometry and texture, serving as a navigable spatial canvas.
- 3D Scanning for Localized Precision: Regions of interest (ROIs), such as intricate emblems or delicate patterns, are identified via user input (e.g., curator guidance) or algorithmic detection. These areas are then scanned at sub-millimeter resolution using structured-light scanning producing high-LOD mesh fragments.

This hybrid workflow addresses three critical challenges in heritage digitization. First, by leveraging 3DGS for base reconstruction, we dramatically accelerate initial processing times compared to full-structure scanning (detailed in Sec. 4.2), enabling scalable digitization of expansive sites like Blickling Hall. Second, the explicit representation of the 3DGS layer preserves the spatial coherence of the entire structure, ensuring that high-resolution regions of interest (ROIs) remain anchored within their original architectural context, a feature absent in fragmented, ROI-centric workflows. Finally, the staged integration of low- and high-LOD data empowers dynamic immersion: visitors fluidly transition from a real-time 3DGS overview to sub-millimeter-accurate meshes within virtual reality (VR), scrutinizing fine details such as plaster tool marks without sacrificing interactivity or spatial awareness. This synergy of efficiency, continuity, and engagement redefines heritage digitization as both a conservation tool and a storytelling medium.

2. Background: Blickling Hall

This section will provide some context on the building of Blickling, the design of the ceiling and its historical significance.

In 1616, Sir Henry Hobart (c.1554-1625), attorney-general and chief justice of the common pleas, purchased the old medieval manor house at Blickling, Norfolk. By 1622 he had poured £6500 into the building of the present magnificent hall, and work on the house's interior would continue after his death until almost the end of the decade [Han08]. Edward Stanyon, a well-known London-based plasterer, was contracted to join the project on 11 August 1620 [SMN86]. His commission was for 'frett ceiling' in the Long Gallery, the Great Chamber, the Withdrawing Chamber, and the Parlour, all of which would be charged at his highest rate, 5s. 6d. a square yard. He tackled the Long Gallery first. Described by Claire
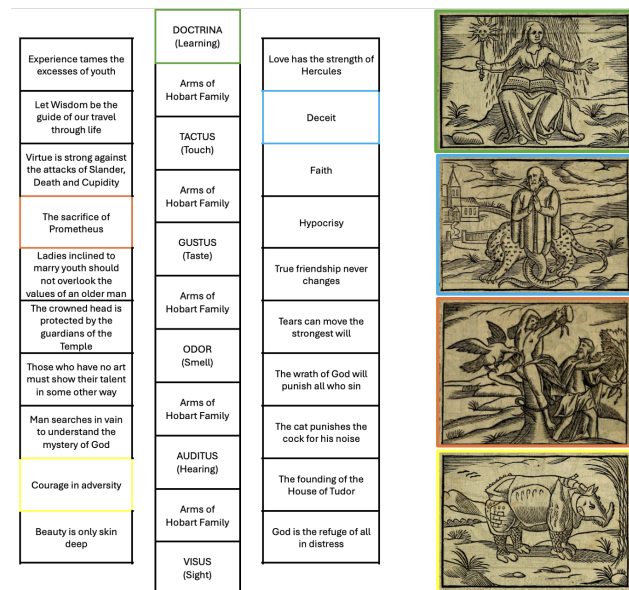

Figure 2: *Layout of emblems on the ceiling. The 'Doctrina' and the 20 emblems around the left and right sides of the ceiling are drawn from the image source: Henry Peacham's Minerva Britanna (1612) [Pea12].*

Gapper as 'a tour de force of Jacobean plasterwork at its most elaborate', the ceiling consists of a series of emblems [Gap98] (Fig. 2). Running through the centre of the room are the Five Senses, culminating at the far end of the Long Gallery with an emblem of 'Doctrina' - Learning. The implication is of a journey through the senses, capable perhaps of both Aristotelian (learning is achieved through the senses) and Platonic (learning is achieved by transcending them) interpretations. The Five Senses were themselves popular themes in Renaissance homes of the period - a painted version can be found at Knole House in Kent [Ban23]. In between the senses, also in the centre of the ceiling, are five iterations of the arms of Sir Henry Hobart. Around the left and right sides of the ceiling are a further series of 20 emblems, each with its own Latin motto and gnomic, allegorical or mythological figures, drawn from Henry Peacham's Minerva Britanna (published 1612, and also the source for the image of 'Doctrina').

The intermedial transformation of the rather crude woodcuts in Peacham's book into the wonderfully simple and elegant designs for the plasterwork was itself a considerable creative endeavour. The essential idea, however, of decorating a house with sententious sayings or visual emblems was not unusual. But whereas women's examples were often associated with private, enclosed household spaces, suitable for women's meditation according to early modern gender expectations, Blickling's are displayed in a strikingly public space. Long Galleries became showpiece features of late sixteenth- and seventeenth-century English grand houses. They were designed as places of show for visitors, who could promenade up and down the Gallery with magnificent views of the land outside over which the lord of the house held sway. Emblems, viewed in this context, provided opportunities for moral exercise to accom-

pany the physical exercise of promenading the Gallery [Ads20]. But they also provided opportunities for conversation, to show off a visitor's wit and ingenuity in decoding the emblems, or for the master of the house to demonstrate the depth of his lifelong worldly wisdom. There is some evidence that the books from which the emblems were sourced would have been on hand to guide interpretation. Each of Peacham's emblems is accompanied by a poem that helps to clarify the emblem's meaning. Perhaps the exercise was to get as close as possible to Peacham's interpretation; or perhaps it was to depart plausibly and elegantly from it.

The range of emblems chosen from Peacham's book furnish all these opportunities. Appropriately for the emblem, which sets up a contrast between what it shows and what it means, many meditate on duplicity: 'Personam non animum' (not the mask, but the soul), 'Dolus' (deceit), or 'Pulchritudo faeminea' (Feminine beauty), where a woman holding a mirror sits on a dragon. This theme of duplicity hints at a life spent navigating the realm of courtly power, which is hinted most explicitly in 'Tyranni Morbus Suspicio' (Suspicion is the disease of the tyrant), which feels like a fashionably Senecan or Tacitean political maxim (brought into vogue by Justus Lipsius). A very few emblems are explicitly Christian, such as 'Deus Ultimum Refugium' (God the last refuge), others Christianise classical myth, such as 'Omnis a Deo Sapientia' (All Wisdom is from God), which accompanies a 'wonderfully naive rendering' of the birth of Minerva (wisdom) from Jove's head [JS89]. At least one emblem's significance is radically different according to Peacham's book than anything which the viewer might expect. 'Sed adhuc mea messis in herba est' (But my harvest is not yet come) accompanies agricultural implements, perhaps implying a sense of youthful potential and future promise. Some might identify the quotation as from Ovid's Heroides, in which Helen rebuffs the advances of Paris (XVI.263). Peacham, however, takes this in a surprising and scurrilously satirical direction. His emblem is addressed 'to a certain noble Italian woman of about fifty years old, who not so long ago married a boy scarcely 15 years old' [Pea12]. Stanyon's emblematic ceiling, therefore, offers not so much straightforward moral exercises to Hobart's visitors, as a teasing hermeneutic game in which they might participate on several different levels.

The remodelling of Blickling by Norwich architect Thomas Ivory in the 1760s saw the loss of Stanyon's plaster ceiling for the Withdrawing Chamber [SM86]. Even if such remodelling is now no longer a threat, the loss of Stanyon's work even over time in Blickling itself points to the fragility of this kind of artistic treasure and the need for digital preservation. Moreover, while Stanyon's masterpiece does survive, the setting of the Long Gallery - from which, we have seen, its meaning is inseparable - has been radically transformed. In the 1740s, Blickling's custodian at that time, John Hobart (1693-1756), 1st Earl of Buckinghamshire, inherited a substantial library of 10,000 books from Sir Richard Ellys (1688?-1742), a learned Non-Conformist with a house in London and strong family ties to Lincolnshire [Pur19]. As such, the Long Gallery was transformed into a magnificent library, but one which drew educated conversational focus away from the emblematic ceiling and towards the spines on the shelves. Digital heritage and VR therefore promises not only to preserve the ceiling but also to reconnect viewers to it in a way that has not been possible for nearly three cen-

turies, immersing them once again in the interpretative challenges and pleasures offered by the ceiling.

3. Related Work

3.1. Ceiling Digitization in Cultural Heritage

MacDonald et al. [MGRVM12] [MHAR14] worked on monitoring and visualizing damage on the painted ceiling of Hampton Court Palace's Queen's Staircase. Their methodology employed photometric stereo techniques using a fixed camera position with multiple flash lighting angles to generate detailed 3D surface maps capable of detecting surface deformations, cracks, and flaking paint with a remarkable depth resolution of 0.2mm. This non-invasive approach achieved results comparable to expensive 3D laser scanners while using relatively affordable equipment and causing minimal disruption to the site.

Guarneri et al. [GCC*19] used a multi-wavelength 3D laser scanning system to digitize the frescoed ceiling "The Triumph of Divine Providence" in Palazzo Barberini, Rome. The authors describe how their system overcomes several challenges typically encountered in large-scale cultural heritage digitization, including varying ambient lighting, long scanning distances, and the need to avoid scaffolding. Instead of relying on a single laser plus a coaxial camera, their multi-wavelength scanning approach utilizes three amplitude-modulated laser sources and lock-in amplifiers to capture both color and distance information with minimal interference from environmental light.

Reinoso-Gordo et al. [RGGGBO21] made digital documentation of a 16th-century wooden ceiling with geometric interlacing patterns in the Pinelo Palace in Seville. They combined two digital techniques: 3D laser scanning for precise metric data on deformations and photogrammetry for high-resolution visualization of intricate details. This dual methodology enabled them to quantify structural issues while preserving the ceiling's artistic and historical features. The authors demonstrated how digital documentation serves as both a preservation tool and a scientific foundation for future restoration efforts, particularly for ceilings suffering from significant deformation.

3.2. 3D Scanning for Heritage Digitization

3D scanning has revolutionized cultural heritage preservation for decades by enabling non-invasive, high-fidelity capturing. Laser scanning and structured-light scanning, initially developed for industrial quality control and reverse engineering, have been adapted to heritage contexts for their ability to document complex geometries with sub-millimeter precision. Remondino extensively reviewed the capabilities and constraints of optical sensors, presenting practical examples of their successful application in heritage documentation [Rem11].

A survey by Scopigno et al. [SCP*17] provides an extensive overview of digital fabrication methods, specifically focusing on 3D scanning and printing technologies and their applications within the domain of cultural heritage preservation. Despite their versatility, for some applications, the geometry of artifact surfaces cannot be fully captured using laser or structured light scanning techniques, necessitating alternative methods. For example, Laycock et

al. [LBM*13] presented an approach employing X-Ray Micro-CT technology to effectively capture intricate and occluded details in the base of a 19th-century Cantonese chess piece model.

Nonetheless, traditional 3D scanning workflows for large-scale heritage scenes remain labor-intensive and time-consuming. Such limitations validate the need for adaptive workflows like our Level-of-Detail framework, which combines rapid 3D Gaussian Splatting for global reconstruction with targeted 3D scanning of regions of interest, optimizing both the accuracy and efficiency of heritage digitization.

3.3. 3D Gaussian Splatting Reconstruction

3D Gaussian Splatting (3DGS) [KKLD23] has emerged as a transformative technique in 3D reconstruction, offering real-time rendering and high fidelity through explicit anisotropic Gaussian representations. Subsequent studies, such as [KSE*25] and [QXLH25], explored 3DGS's applicability in Virtual Reality (VR), showing its potential for immersive virtual environments. Recent research also highlights the growing versatility of 3DGS in cultural heritage applications. At the site scale, Yu et al. [YVvOP25] integrate UAV imagery with 3DGS to document large modern-heritage buildings, achieving high geometric accuracy while enabling real-time photorealistic VR walkthroughs. At the object scale, Dahaghin et al. [DCR*24] demonstrate that a smartphone-only pipeline, combined with a GS-based segmentation strategy, can produce clean, per-artifact meshes from museum photo sets without manual masking. Complementing these technically focused efforts, Jamil and Brennan [JB25] adopt a phenomenological perspective, emphasizing how the unique visual aesthetic of 3DGS enhances the sense of presence and memory in immersive heritage experiences. In this paper, we further demonstrate the suitability of 3DGS for heritage digitization in VR, particularly in challenging indoor environments with distant and elevated features.

4. Multimodal Data Acquisition

4.1. Video Acquisition

We implemented non-invasive photographic survey to document the whole ceiling, eliminating the need for scaffolding while minimizing disruption to Blickling Hall's daily operations.

The ceiling was recorded in 4K resolution (3840 × 2160 pixels) using an iPhone 12 equipped with an Ultra Wide Camera (13 mm, f/2.4) at 60 fps. The video documentation includes twelve complete passes along the full length of the ceiling, captured from two different heights and at various tilted angles. The total recording duration was 18 minutes and 51 seconds (Fig. 3). The video was subsampled at 1 fps using FFmpeg, yielding 1131 frames for photogrammetric processing. These images were processed through Structure-from-Motion (SfM) [SF16] to generate a sparse point cloud and camera calibration (Fig. 3), which served as the initialization for 3DGS reconstruction (detailed in Sec. 5.1).

4.2. 3D Scanning

In this work we used the Artec Eva structured light scanner to obtain high resolution triangle meshes to represent key features of
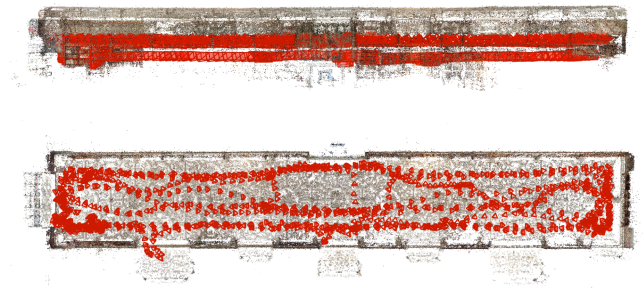

Figure 3: *Camera pose estimation and sparse point cloud initialization. (Top) Side view of the capture setup at two different heights, with the camera positioned approximately 1 m and 2 m beneath the ceiling. (Bottom) Overhead trajectory visualization showing 12 complete passes. Path deviations reflect our non-invasive protocol that avoided furniture displacement at Blickling Hall during documentation.*

Figure 4: *3D Scanning of features in the ceiling of the Long Gallery in Blickling Hall. An Artec Eva is attached to an extended telescopic tripod to get the scanner within 0.4 to 1m range of the ceiling and it is scanned whilst viewing the capture area on an laptop. This is achieved with two people to ensure free movement of scanner and laptop whilst capturing.*

ROIs in the ceiling. This scanner is capable of an accuracy up to 0.1mm and a resolution up to 0.2mm with a capture rate of up to 16fps. A telescopic tripod was used to get the Artec Eva to a distance between 0.4 to 1m from the surface of the ceiling as required for effective scanning. We used the Artec Studio software to monitor the distance the scanner was to the ceiling during scanning and the colour-coded images in the software provides a very helpful visual cue to maintain the correct distance to objects. During scanning the typical distance between the scanner and the ceiling was in the range 0.6 to 0.75m. The approach to stand on the floor with the extended tripod was taken due to health and safety concerns around our use of any form of ladder or scaffolding tower within the site. It was noted that any higher ceilings would begin to require support

for working closer to the ceiling due to the limited cable lengths. The ability to scan with the Eva on such an extended telescopic tripod, however, was surprisingly effective at capturing the surface details of the ceiling. By watching the area being targeted by the scanner on the laptop screen the scanner was moved over the entire capture area (Fig. 4).

Once the scanning was complete the Artec Studio tools were used to produce the surface mesh using the Sharp Fusion technique (with a resolution of one and maximum hole radius of five). Some surface errors did occur, particularly around very concave areas, and these were removed using the defeature brush. 3D models in OBJ file format were then exported (Fig. 5).

Figure 5: *Sub-millimeter-accurate digital documentation of the 'Odor' emblem (representing smell among the five senses) reveals intricate surface details in this central ceiling motif. The textured mesh faithfully preserves the craftsmanship while enabling non-contact study.*

5. Level-of-Detail Framework

Our LOD framework combines 3DGS for efficient low-LOD ceiling reconstruction (Sec. 5.1) with adaptive ICP alignment of high-LOD scanned regions (Sec. 5.2), enabling real-time VR exploration with smooth transitions between global views and detailed inspection of intricate features (Sec. 5.3).

5.1. 3DGS Reconstruction

The input to 3D Gaussian Splatting (3DGS) comprises a collection of images capturing a static scene, accompanied by camera poses and a sparse point cloud reconstructed via Structure-from-Motion (SfM) [SF16] (see Sec. 4.1 for details). These points are used to initialize a set of 3D Gaussians, each defined by a mean (position) $\mu \in \mathbb{R}^3$, covariance $\Sigma \in \mathbb{R}^{3 \times 3}$, color c, and opacity α. This representation yields a compact yet expressive model of the 3D scene, where anisotropic volumetric splats can render fine geometric details by rasterization. The shaded color $C(u)$ for pixel u is computed via α-blending:

$$C(u) = \sum_{i=1}^{N} T_i\, g_i^{2D}(u)\, \alpha_i\, c_i, \quad T_i = \prod_{j=1}^{i-1}\left(1 - g_j^{2D}(u)\,\alpha_j\right), \quad (1)$$

where T_i is the transmittance term, α_i is opacity, c_i is the view-dependent color modeled by Spherical Harmonics (SH), and $g_i^{2D}(u)$ is the 2D Gaussian kernel defined by 3D-to-2D projection.

The 3D Gaussian parameters are projected to screen space using camera extrinsics $W \in \mathbb{R}^{4 \times 4}$ and intrinsics $K \in \mathbb{R}^{3 \times 3}$:

$$\mu' = KW\begin{bmatrix}\mu \\ 1\end{bmatrix}, \qquad\qquad (2)$$

$$\Sigma' = JW\Sigma W^\top J^\top, \qquad\qquad (3)$$

where J is the Jacobian of the perspective projection, and μ', Σ' are the projected 2D parameters. Then the projected 2D Gaussian is defined as:

$$g^{2D}(u) = \exp\left(-\frac{1}{2}(u - \hat{\mu}')^\top \hat{\Sigma}'^{-1}(u - \hat{\mu}')\right), \qquad (4)$$

where $\hat{\mu}'$ and $\hat{\Sigma}'$ are the normalized screen-space coordinates.

The total loss function to train the 3D Gaussians combines color term $\mathcal{L}_{\text{color}}$ and regularization term $\mathcal{L}_{\text{reg}}$. Here, $\mathcal{L}_{\text{reg}}$ penalizes excessive Gaussian size, opacity, and covariance rank to maintain a compact representation. $\mathcal{L}_{\text{color}}$ includes L1 color loss and SSIM (Structural Similarity Index Measure) loss, following the original 3DGS formulation [KKLD23]:

$$\mathcal{L}_{\text{color}} = \sum_{u \in \mathcal{R}} \|C(u) - C_{\text{gt}}(u)\|_1 + \lambda_{ssim}\mathcal{L}_{\text{SSIM}}(u), \qquad (5)$$

where $\mathcal{R}$ contains all valid pixels and $C_{\text{gt}}(u)$ is the ground truth color. s In preliminary experiments on the long ceiling scene, a large and unbounded environment, we observed artifacts such as Gaussians 'floating' in unobserved regions. To address this, we introduced an additional depth loss $\mathcal{L}_{\text{depth}}$ (implemented via gsplat [YLK*24]), which anchors Gaussians to geometrically validated depths derived from the input data. The rendered depth $D(u)$ is computed similarly:

$$D(u) = \sum_{i=1}^{N} T_i\, g_i^{2D}(u)\, \alpha_i\, d_i, \qquad\qquad (6)$$

where d_i is the depth of the i-th Gaussian's mean in camera coordinates. The depth loss $\mathcal{L}_{\text{depth}}$ is set to a similar L1 form:

$$\mathcal{L}_{\text{depth}} = \sum_{u \in \mathcal{M}} \|D(u) - D_{\text{gt}}(u)\|_1. \qquad\qquad (7)$$

Using the depth-regularized 3DGS framework, we successfully reconstructed the entire 37.5-meter-long ceiling in Blickling Hall's Long Gallery. The depth constraints enabled efficient training of compact Gaussians for this unbounded scene, yielding a final model with 3,023,022 Gaussians after 30,000 training epochs and subsequent refinement using SuperSplat [Pla24] Fig. 6 demonstrates the rendering quality through an evaluation view, including its corresponding depth map visualization. The metrical evaluation of whole ceiling reconstruction will be discussed in Sec. 6.

Figure 6: *View (middle) and depth (bottom) renderings from 3D Gaussian Splatting trained by depth-regularized framework. PSNR: 22.16 dB, SSIM: 0.7015, LPIPS: 0.5427 against evaluation frame (top).*

5.2. Scanned Mesh Alignment

The Iterative Closest Point (ICP) algorithm is widely used for geometric alignment of 3D models when an initial relative pose estimate is available [RL01]. Numerous ICP variants have been proposed, modifying key components such as point selection, correspondence matching, and error minimization. A common variant is the Point-to-Plane ICP [CM92], which leverages surface normals for improved convergence.

We developed an inverse ICP alignment scheme leveraging accurate normals from high-resolution scans (e.g., the scanned 'Arms of the Hobart Family' emblem, Fig. 7). Initialized by matching a cropped sparse point cloud (approx. 50,000 points) to the dense mesh (601,702 faces, 300,725 vertices), our point-to-plane ICP iteratively solves for transformations until convergence. The final inverse transformation aligns the dense mesh to the full 3DGS point cloud, as formalized in Table 1. The alignment *Arms of Hobert*
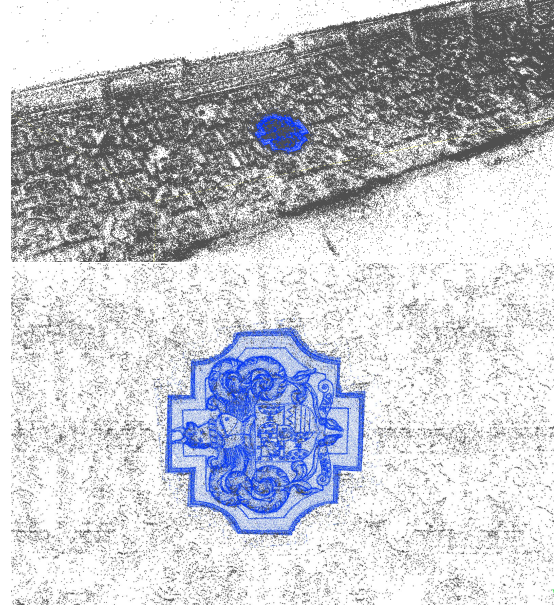

Figure 7: *ICP Alignment of the 'Arms of the Hobart Family' emblem to 3DGS point cloud.*

Family mesh against the point cloud has a Root Mean Squared Error (RMSE) of 0.0020 meters computed over 50,000 points. On average, the alignment of all scanned emblems have an average RMSE of 0.0029 meters.

Table 1: *Trimmed Sparse-to-Dense ICP with Inverse Alignment*

Description
Input: Full sparse cloud $\mathcal{X}_{\text{full}} = \{\mathbf{x}_i\}$, dense mesh $\mathcal{Y}_{\text{dense}}$ with normals $\{\mathbf{n}_j\}$, bounding box $\text{BBox}(\mathcal{Y}_{\text{dense}})$
Preprocess:
$\quad \mathcal{X}_{\text{trim}} \leftarrow \text{Crop}(\mathcal{X}_{\text{full}}, \text{BBox}(\mathcal{Y}_{\text{dense}}))$
$\quad \mathcal{Y}_{\text{points}} \leftarrow \text{SampleVertices}(\mathcal{Y}_{\text{dense}})$
Initialize: $\mathbf{R} \leftarrow \mathbf{I}$, $\mathbf{t} \leftarrow \mathbf{0}$, error $\leftarrow \infty$
Repeat:
$\quad$ Find correspondences: $\mathcal{C} \leftarrow \{(\mathbf{x}_i, \mathbf{y}_j, \mathbf{n}_j) \mid \mathbf{y}_j = \text{NN}(\mathbf{R}\mathbf{x}_i + \mathbf{t}, \mathcal{Y}_{\text{points}})\}$
$\quad$ Build linear system:
$\quad\quad \mathbf{A}_i = [(\mathbf{x}_i \times \mathbf{n}_j)^\top \quad \mathbf{n}_j^\top], \mathbf{b}_i = -\mathbf{n}_j^\top (\mathbf{x}_i - \mathbf{y}_j)$
$\quad$ Solve for incremental transformation:
$\quad\quad \mathbf{T} = (\mathbf{A}^\top \mathbf{A})^{-1} \mathbf{A}^\top \mathbf{b}$, where $\mathbf{T} = [\delta\theta^\top \quad \delta\mathbf{t}^\top]^\top$
$\quad$ Update transformation: $\mathbf{R} \leftarrow (\mathbf{I} + [\delta\theta]_\times)\mathbf{R}$, $\mathbf{t} \leftarrow \mathbf{t} + \delta\mathbf{t}$
$\quad$ Compute error: error $\leftarrow \frac{1}{N} \sum \|\mathbf{n}_j^\top (\mathbf{R}\mathbf{x}_i + \mathbf{t} - \mathbf{y}_j)\|^2$
Until: error < threshold or max iterations
Invert: $\mathbf{T}_{\text{final}} = \begin{bmatrix} \mathbf{R}^\top & -\mathbf{R}^\top \mathbf{t} \\ \mathbf{0}^\top & 1 \end{bmatrix}$
Return: Final transformation $\mathbf{T}_{\text{final}}$ aligning $\mathcal{Y}_{\text{dense}} \rightarrow \mathcal{X}_{\text{full}}$

In the pseudocode, $\mathbf{R} \in \text{SO}(3)$ is rotation matrix, $\mathbf{t} \in \mathbb{R}^3$ is translation vector, $\text{NN}(\cdot)$ is Nearest-neighbor function that maps a point
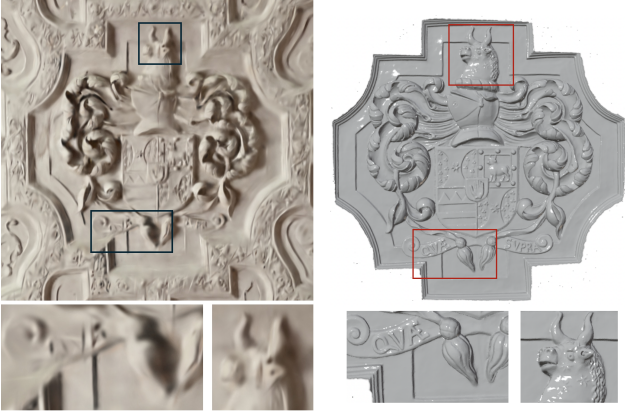
Figure 8: *Comparison of fine details in 3DGS rendering and the high-fidelity scanned mesh.*

Figure 9: *VR LOD System. Users can navigate and interact with patterns on the 3DGS ceiling (top). When a pattern is selected, the aligned emblem mesh appears (middle), triggering an animation that brings it into the near-eye field for detailed viewing accompanied by storytelling elements (bottom).*

in $\mathcal{X}$ to its closest match in $\mathcal{Y}$. $\mathbf{A}_i \in \mathbb{R}^{1 \times 6}$ is linearized constraint matrix for the i-th correspondence, $\mathbf{b}_i \in \mathbb{R}$ is residual term for the i-th correspondence. $\mathbf{T} \in \mathbb{R}^6$ is incremental transformation parameters, $\mathbf{T} = [\delta\theta^\top \; \delta\mathbf{t}^\top]^\top$. $\delta\theta \in \mathbb{R}^3$ is incremental rotation vector (angle-axis representation), and $\delta\mathbf{t} \in \mathbb{R}^3$ is incremental translation vector. $[\delta\theta]_\times$ is a skew-symmetric matrix form of $\delta\theta$, used to approximate small rotations:

$$[\delta\theta]_\times = \begin{bmatrix} 0 & -\delta\theta_z & \delta\theta_y \\ \delta\theta_z & 0 & -\delta\theta_x \\ -\delta\theta_y & \delta\theta_x & 0 \end{bmatrix}.$$

5.3. LOD Visualization in Virtual Reality

By combining the 3DGS reconstruction of the entire 37.5-meter ceiling with high-resolution 3D scans of emblematic patterns, we developed a hybrid visualization system for Virtual Reality. The necessity of our LOD approach is demonstrated through comparative analysis in Fig. 8. Using depth-aware 3DGS, we efficiently reconstructed the full ceiling from 1131 photographs captured with a mobile camera (Sec. 4.1), achieving rapid processing and good overall quality while sacrificing some fine details important for immersive viewing and digital preservation. To bridge this gap, we integrated submillimeter-accurate 3D meshes of the emblematic elements, enabling immersive near-eye examination and direct interaction with intricate details that would remain inaccessible either during in-situ observation or in VR without LOD framework.

Our VR system implements carefully choreographed animations and intuitive interaction mechanics to smoothly transition emblematic elements from their ceiling-mounted positions to near-eye examination distance. This design enables fluid scaling between architectural context views and immersive close-up inspection, augmented by narrative storytelling elements (Fig. 9).

The prototype was developed in Unity 6.1, using Meta's XR kit framework to handle VR interactions, with deployment and testing conducted on Meta Quest Pro hardware. It leveraged work from [KSE*25] to render the Gaussian Splat with this tooling.

6. Discussion

Our comparative analysis (Fig.10,11) demonstrates that 3DGS outperforms traditional Multi-View Stereo (MVS) [SZPF16] photogrammetry for elevated ceiling digitization, based on our video-based data collection setup. While both methods begin with sparse point clouds generated via Structure-from-Motion (SfM) [SF16], quantitative results in Table 2 indicate that 3DGS achieves better view reconstruction performance. Crucially, 3DGS enables real-time VR performance (>100 FPS in Unity [KSE*25]) through its lightweight splat-based rendering, avoiding the optimization challenges of dense meshes while maintaining seamless LOD transitions. This performance advantage confirms 3DGS as an ideal so-

lution for creating the spatial canvas in large-scale high ceiling digitization, where it simultaneously achieves geometric accuracy and real-time interactive exploration capabilities.

We also tested video capture using a Sony A7 III DSLR, but it was less suitable for this scene. The Long Gallery Hall has uneven lighting, with illumination primarily from windows on one side. This caused frequent overexposure when facing the windows and underexposure when facing away, leading to loss of ceiling details and inconsistencies that hindered image matching. While manual photo capture with adjusted exposures might help, it was impractical due to the ceiling's height and length. In contrast, the phone camera's 4K HDR video offered better dynamic range, yielding more balanced lighting and finer details throughout the scene.

We further employed 3D printing to evaluate the fidelity of selected scanned models (Sec. 4.2). To prepare the models for physical printing, we converted the geometry into watertight solids using 3DS Max by extruding surfaces and capping holes. A slice plane was applied to create a flat base for stability during printing. The final 3D prints (Fig. 12) were produced through an online 3D printing service.

Metric	3DGS	MVS+Poisson Meshing
PSNR	21.8379 dB	15.1344 dB
SSIM	0.7988	0.6412
LPIPS	0.4639	0.4365

Table 2: *Comparison of performance metrics between 3DGS and MVS+Poisson Mesh calculated on a withheld evaluation set.*

7. Conclusion

Tested on Blickling Hall's Long Gallery, we designed a hybrid workflow for scalable level-of-detail digitization tailored to the challenges of high ceiling and large scene. The workflow operates in two stages: first, 3D Gaussian Splatting provides a coarse reconstruction that captures global geometry and texture, serving as a navigable spatial canvas; second, high-resolution 3D scanning targets emblematic regions to produce sub-millimeter meshes for fine-detail inspection and preservation.

This framework demonstrates how an LOD-inspired approach can effectively bridge digital preservation and immersive engagement in large, elevated ceiling environments. We quantitatively evaluated the accuracy of the 3DGS reconstruction and its alignment with high-resolution scans using ICP. Additionally, we compared 3DGS with traditional MVS+Poisson meshing pipelines under our video-based and long-range capture setup, showing that 3DGS achieves better visual and metrical performance. We also discussed the practical benefits of using a smartphone camera to capture HDR video, which offers more balanced lighting and finer detail capture in indoor scenes with uneven illumination.

Beyond this site, the modularity of our workflow allows adaptation to a wide range of heritage contexts, from cathedral domes to archaeological reliefs, supporting both technical scalability and cultural significance.

Future work at Blickling Hall will expand reconstruction to the

Figure 10: *Comparison of 3DGS rendering (top, PSNR: 24.9752 dB, SSIM: 0.7603, LPIPS: 0.5389) and MVS+Poisson Meshing (bottom, PSNR: 17.3688 dB, SSIM: 0.4652, LPIPS: 0.6111) against the original evaluation frame (middle).*

entire Gallery Hall and further optimize lighting conditions for 3DGS capture. We also envision a VR-based puzzle game featuring the emblematic patterns, using technical innovation to enhance public engagement with cultural heritage.

References

[Ads20] ADSHEAD D.: The architectural evolution of picture and sculpture galleries in british country houses, 2020. doi:10.17658/ACH/TE578. 3

[Ban23] BANK K.: "amphions harp gaue sence vnto stone walles":

Figure 11: *Comparisons of 3DGS (top, left) and MVS+Poisson Meshing (bottom, right) reconstruction of the whole ceiling in low-LOD.*

Figure 12: *3D printing prototypes of the scanned 'Odor'(Smell) and 'Arms of Hobart Family' models.*

The five senses and musical–visual affect. *Arts 12*, 5 (2023). URL: https://www.mdpi.com/2076-0752/12/5/219, doi: 10.3390/arts12050219. 2

[CM92] CHEN Y., MEDIONI G.: Object modelling by registration of multiple range images. *Image and Vision Computing 10*, 3 (1992), 145–155. Range Image Understanding. doi:https://doi.org/10.1016/0262-8856(92)90066-C. 6

[DCR*24] DAHAGHIN M., CASTILLO M., RIAHIDEHKORDI K., TOSO M., DEL BUE A.: Gaussian heritage: 3d digitization of cultural heritage with integrated object segmentation. *arXiv preprint arXiv:2409.19039* (2024). 4

[Gap98] GAPPER C.: *Plasterers and Plasterwork in City, Court and Country c.1530–c.1660.* PhD thesis, Courtauld Institute of Art, 1998. Discussion of Blickling and Stanyon at https://clairegapper.info/plasterers-company.html. Biographical Dictionary of London Plasterers 1550–1625: STANYON, Edward (1581–1632/3) at https://clairegapper.info/gazetteer-of-plasterers-s.html. URL: https://clairegapper.info. 1, 2

[GCC*19] GUARNERI M., CECCARELLI S., COLLIBUS M., FRAN-CUCCI M., CIAFFI M.: Multi-wavelengths 3d laser scanning for pigment and structural studies on the frescoed ceiling the triumph of divine providence. *ISPRS - International Archives of the Photogrammetry, Remote Sensing and Spatial Information Sciences XLII-2/W15* (08 2019), 549–554. doi:10.5194/isprs-archives-XLII-2-W15-549-2019. 3

[Han08] HANDLEY S.: Hobart, sir henry, first baronet (c. 1554–1625), lawyer and judge, 01 2008. doi:10.1093/ref:odnb/13391. 2

[HD04] HEOK T. K., DAMAN D.: A review on level of detail. In *Proceedings. International Conference on Computer Graphics, Imaging and Visualization, 2004. CGIV 2004.* (2004), pp. 70–75. doi:10.1109/CGIV.2004.1323963. 2

[JB25] JAMIL O., BRENNAN A.: Immersive heritage through gaussian splatting: A new visual aesthetic for reality capture. *Frontiers in Computer Science 7* (2025), 1515609. 4

[JS89] JACKSON-STOPS G.: A british parnassus: Mythology and the country house. In *The Fashioning and Functioning of the British Country House*, Studies in the History of Art. 1989, pp. 217–238. 3

[KKLD23] KERBL B., KOPANAS G., LEIMKÜHLER T., DRETTAKIS G.: 3d gaussian splatting for real-time radiance field rendering. *ACM Transactions on Graphics 42*, 4 (July 2023). URL: https://repo-sam.inria.fr/fungraph/3d-gaussian-splatting/. 1, 2, 4, 5

[KSE*25] KLEINBECK C., SCHIEBER H., ENGEL K., GUTJAHR R., ROTH D.: Multi-layer gaussian splatting for immersive anatomy visualization. *IEEE Transactions on Visualization and Computer Graphics* (2025), 1–11. URL: https://ieeexplore.ieee.org/document/10919012, doi:10.1109/TVCG.2025.3549882. 4, 7

[LBM*13] LAYCOCK S. D., BELL G. D., MORTIMORE D. B., GRECO M. K., CORPS N., FINKLE I.: Combining x-ray micro-ct technology and 3d printing for the digital preservation and study of a 19th century cantonese chess piece with intricate internal structure. *J. Comput. Cult. Herit. 5*, 4 (Jan. 2013). URL: https://doi.org/10.1145/2399180.2399181, doi:10.1145/2399180.2399181. 4

[LRC*02] LUEBKE D., REDDY M., COHEN J. D., VARSHNEY A., WATSON B., HUEBNER R.: *Level of detail for 3D graphics*. Elsevier, 2002. 2

[MGRVM12] MACDONALD L., GIBB I., ROBSON S., VLACHOU-MOGIRE C.: High art: Visualising damage on a heritage ceiling. In *Electronic Visualisation and the Arts (EVA 2012)* (2012), BCS Learning & Development. 3

[MHAR14] MACDONALD L., HOSSEININAVEH AHMADABA-DIAN A., ROBSON S.: Photogrammetric analysis of a heritage ceiling. *The International Archives of the Photogrammetry, Remote Sensing and Spatial Information Sciences XL-5* (2014), 379–383. URL: https://isprs-archives.copernicus.org/articles/XL-5/379/2014/, doi: 10.5194/isprsarchives-XL-5-379-2014. 3

[Pea12] PEACHAM H.: *Minerva Britanna*. London, 1612. URL: https://archive.org/details/minervabritannao00peac. 1, 2, 3

[Pla24] PLAYCANVAS: Supersplat - 3d gaussian splat editor. https://github.com/playcanvas/supersplat, 2024. 5

[Pur19] PURCELL M.: *The country house library*. Yale University Press, 2019. 3

[QXLH25] QIU S., XIE B., LIU Q., HENG P.-A.: Creating virtual environments with 3d gaussian splatting: A comparative study, 2025. URL: https://arxiv.org/abs/2501.09302, arXiv:2501.09302. 4

[Rem11] REMONDINO F.: Heritage recording and 3d modeling with photogrammetry and 3d scanning. *Remote Sensing 3*, 6 (2011), 1104–1138. URL: https://www.mdpi.com/2072-4292/3/6/1104, doi:10.3390/rs3061104. 3

[RGGGBO21] REINOSO-GORDO J. F., GÁMIZ-GORDO A., BARRERO-ORTEGA P.: Digital graphic documentation and architectural heritage: Deformations in a 16th-century ceiling of the pinelo palace in seville (spain). *ISPRS International Journal of Geo-Information 10*, 2 (2021). URL: https://www.mdpi.com/2220-9964/10/2/85, doi:10.3390/ijgi10020085. 3

[RL01] RUSINKIEWICZ S., LEVOY M.: Efficient variants of the icp algorithm. In *Proceedings Third International Conference on 3-D Digital Imaging and Modeling* (2001), pp. 145–152. doi:10.1109/IM.2001.924423. 6

[SCP*17] SCOPIGNO R., CIGNONI P., PIETRONI N., CALLIERI M., DELLEPIANE M.: Digital fabrication techniques for cultural heritage: a survey. In *Computer graphics forum* (2017), vol. 36, Wiley Online Library, pp. 6–21. 3

[SF16] SCHÖNBERGER J. L., FRAHM J.-M.: Structure-from-motion revisited. In *Conference on Computer Vision and Pattern Recognition (CVPR)* (2016). 4, 5, 7

[SM86] STANLEY-MILLSON C.: Blickling hall: The building of a great house. *Journal of the Royal Society for the Encouragement of Arts, Manufactures and Commerce 135*, 5365 (Dec 01 1986), 58. URL: https://www.proquest.com/scholarly-journals/blickling-hall-building-great-house/docview/1307309858/se-2. 3

[SMN86] STANLEY-MILLSON C., NEWMAN J.: Blickling hall: The building of a jacobean mansion. *Architectural History 29* (1986), 1–42. doi:10.2307/1568500. 2

[SZPF16] SCHÖNBERGER J. L., ZHENG E., POLLEFEYS M., FRAHM J.-M.: Pixelwise view selection for unstructured multi-view stereo. In *European Conference on Computer Vision (ECCV)* (2016). 7

[YLK*24] YE V., LI R., KERR J., TURKULAINEN M., YI B., PAN Z., SEISKARI O., YE J., HU J., TANCIK M., KANAZAWA A.: gsplat: An open-source library for Gaussian splatting. *arXiv preprint arXiv:2409.06765* (2024). URL: https://arxiv.org/abs/2409.06765, arXiv:2409.06765. 5

[YVvOP25] YU Y., VERBREE E., VAN OOSTEROM P., POTTGIESSER U.: 3d gaussian splatting for modern architectural heritage: Integrating uav-based data acquisition and advanced photorealistic 3d techniques. *AGILE: GIScience Series 6* (2025), 51. URL: https://agile-giss.copernicus.org/articles/6/51/2025/, doi:10.5194/agile-giss-6-51-2025. 4